International Journal of Innovative Computing, Information and Control
Volume **9**, Number **2**, February **2013**

ICIC International ©2013 ISSN 1349-4198
pp. **651–666**

OPTIMAL FUZZY GAIN SCHEDULING OF PID CONTROLLER OF SUPERCONDUCTING MAGNETIC ENERGY STORAGE FOR POWER SYSTEM STABILIZATION

Theerawut Chaiyatham and Issarachai Ngamroo

School of Electrical Engineering
Faculty of Engineering
King Mongkut's Institute of Technology Ladkrabang
Chalongkrung Road, Ladkrabang, Bangkok 10520, Thailand
ngamroo@gmail.com

Received October 2011; revised February 2012

Abstract. *It is well known that the proportional-integral-derivative (PID) can be applied to solve practical control problems effectively. However, in the face of the high system nonlinearity, the PID controller with fixed parameters may fail to provide satisfactory control performance. To enhance the PID control effect, a new design of the fuzzy gain scheduling of PID controller (FGS-PID) is presented in this paper. The proposed technique is applied to design FGS-PID controllers of superconducting magnetic energy storage (SMES) for power system stabilization. Without trial and error, the scale factors, membership functions and control rules of the FGS-PID controller are automatically tuned by a bee colony optimization. With the optimal FGS-PID controller, the PID parameters can be adjusted automatically according to various system operating conditions. As a result, the high robustness of the FGS-PID controller can be expected. Simulation study confirms that the stabilizing effect and robustness of the proposed SMES with an optimal FGS-PID controller are much superior to those of the SMES with an optimal PID controller.*

Keywords: Fuzzy gain scheduling, PID controller, Power system stabilization, Superconducting magnetic energy storage, Bee colony optimization

1. **Introduction.** With the development of power systems around the world, the construction of extensive interconnected lines among different power systems has considerably increased. The interconnection of power systems not only provides the high system reliability, but also increases the economical merits significantly. Nevertheless, the increase in interconnected power systems has brought a low frequency inter-area oscillation with poor damping [1]. The inter-area oscillation may cause the system instability and complete blackout eventually. To damp out the inter-area oscillations, several devices have been applied in previous works such as power system stabilizer [2], thyristor controlled series capacitor [3] and static var compensator [4].

Among the stabilizing devices, the superconducting magnetic energy storage (SMES) which can rapidly supply/absorb electrical power to/from the power systems, is expected as the smart stabilizing device [5]. The simultaneous active and reactive power controls of SMES can be applied as a channel to mitigate the problem of inter-area oscillations due to undesirable disturbances. In [6], the robust damping controller design of SMES based on a weight and normalized eigenvalue-distance minimization method has been presented. In [7], a linear matrix inequality approach to robust damping control design in power systems with SMES has been proposed. In [8], the SMES controller based on H_∞ loop shaping control has been applied to stabilize system frequency oscillation. In

[9], the robust SMES controller based on H_∞ loop shaping control has been proposed to stabilize the inter-area oscillation. In [10], a robust mixed H_2/H_∞ control for frequency stabilization of an interconnected power system including SMES has been studied. In [11], the robust pole placement design of SMES controller for damping inter-area oscillations has been presented. Even the SMES controllers proposed in [6-11] are able to solve the problem of inter-area oscillation successfully, the structure of these SMES controllers is complex with high order which is not easy to implement in practical systems.

Generally, the most popular controller used in industrial systems is the proportional-integral-derivative (PID) controller because it has a simple structure and a high ability of solving many practical control problems [12,13]. The utilizations of PID controller have been proposed in many research works. In [14], a new design of a performance-adaptive PID controller with model prediction structure has been proposed. An optimal PID controller design for a class of PWM feedback time-varying systems by fusing the orthogonal-functions approach and the genetic algorithm has been studied in [15]. A PID controller plus a novel linear-to-nonlinear translator has been proposed and applied to improve the operating performance of the boost converter [16]. A unified PID tuning method for load frequency control of power systems has been discussed in [17]. However, under the high nonlinearity of the system, a PID controller with fixed parameters may no longer provide satisfactory control performance, since the PID parameters should be adjusted following a change of input signal [18].

To enhance the control performance of the PID controller against high system nonlinearity, the application of knowledge systems such as fuzzy control [19-21] and fuzzy gain scheduling control [22] has been proposed. There are many previous research works which have applied the fuzzy gain scheduling control to improve the controller performance by varying the control parameters according to the input signal. In [23], a fuzzy application to load-frequency control using fuzzy gain scheduling of PI controllers has been proposed. In [24], a fuzzy gain scheduling PI controller has been applied to an interconnected electrical power system. In [25], an application of fuzzy gain-scheduling proportional-integral control has been proposed to improve engine power and speed behavior in a hybrid electric vehicle. In [26], a fuzzy gain scheduling integral and derivative controller has been applied to automatic generation control of power system. It seems that these works can show the effectiveness of fuzzy gain scheduling to improve the controller. Nevertheless, these papers have been proposed without considering the optimal design of the fuzzy parameters although the selection of scale factors (SF), membership functions (MF) and control rules (CR) of the fuzzy gain scheduling is very important procedure.

To overcome this problem, this paper presents a new design of optimal fuzzy gain scheduling of PID (FGS-PID) controller for the SMES to stabilize the power system oscillation. To achieve the optimal SFs, MFs and CRs of the FGS-PID controller, a bee colony optimization (BCO) [27] is applied. Simulation study is carried out in the nonlinear model of a two-area four-machine interconnected power system. The proposed SMES with an optimal FGS-PID controller not only shows superior damping effect to the SMES with an optimal PID controller, but also provides high robustness under various operating conditions and large disturbances.

2. **Study Power System and SMES Model.** A two-area four-machine interconnected power system [1] in Figure 1 is used as the study system. Two areas are connected by an AC tie-line which exhibits a weak inter-area oscillation. Each area has two generators, i.e., G1 and G2 in area 1, and G3 and G4 in area 2. Each generator is represented by the fourth-order model and is equipped with a simplified exciter and governor [1]. For

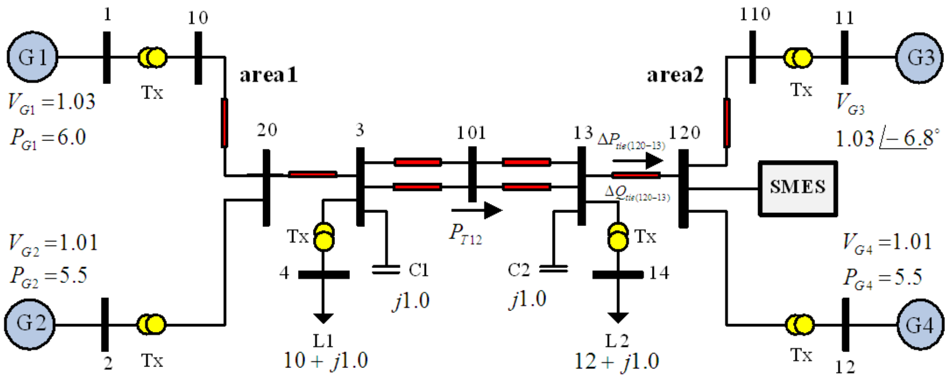

FIGURE 1. Two-area interconnected power system with SMES

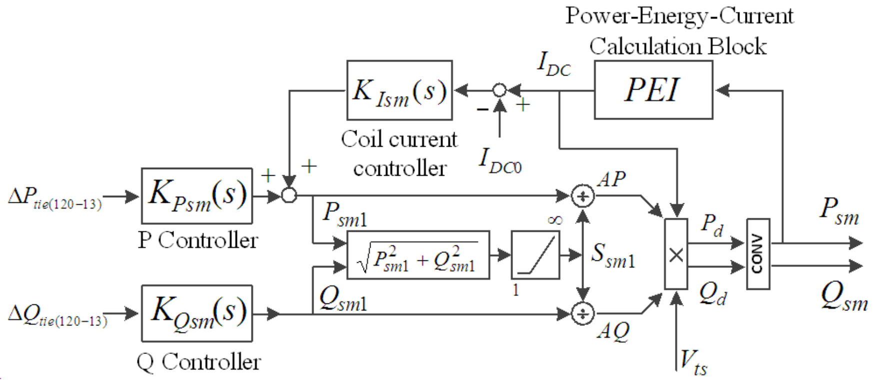

FIGURE 2. SMES model with active and reactive controllers

the study purpose, the active power (P_{T12}) is transferred from areas 1 to 2. Based on the residue method [7], the suitable location of SMES is selected at bus 120 in area 2.

The SMES model with active and reactive power modulation control scheme, as depicted in Figure 2, is used here [28]. In particular, the SMES unit includes active power (P) controller ($K_{Psm}(s)$) and reactive power (Q) controllers ($K_{Qsm}(s)$). The active and reactive power flow deviations from bus 120 to bus 13 ($\Delta P_{tie(120-13)}$ and $\Delta Q_{tie(120-13)}$) are used as the feedback input signals for the SMES controller.

The effect of SMES coil current (I_{DC}) is also included in this model, since the dynamic behaviour of I_{DC} affects the overall performance of SMES. In practice, I_{DC} is not allowed to reach zero to prevent the possibility of discontinuous conduction under unexpected disturbances. On the other hand, I_{DC} which is above the maximum allowable limit may lead to the loss of superconducting properties. On the basis of the hardware operational constraints, the lower and upper coil current limits are considered and assigned as $0.30I_{DC0}$ and $1.38I_{DC0}$, respectively [28], where I_{DC0} is an initial value of I_{DC}. In addition, the coil current controller $K_{Ism}(s)$ in Figure 2 which is a proportional-integral controller, is used for stabilizing the SMES coil current. Here, I_{DC} can be calculated from the Power-Energy-Current (PEI) block which has a relation as

$$I_{DC} = \sqrt{I_{DC0}^2 - 2E_{out}/(L_{sm}I_{sm,base}^2)} \tag{1}$$

$$E_{out} = \int P_{sm}dt.S_{sm,base} \tag{2}$$

where E_{out} is the SMES energy output (J), L_{sm} is the SMES coil inductance (H), $I_{sm,base}$ is the SMES current base (A) and $S_{sm,base}$ is the SMES MVA base (MVA). Subsequently, the energy stored in an SMES unit (E_{sm}) and the initial energy stored (E_{sm0}) can be determined by

$$E_{sm} = E_{sm0} - E_{out} \tag{3}$$

$$E_{sm0} = 0.5 L_{sm} I_{sm0}^2 I_{sm,base}^2. \tag{4}$$

The desired active (P_d) and reactive (Q_d) power outputs of SMES can be expressed as

$$P_d = V_{ts} I_{DC} AP \tag{5}$$

$$Q_d = V_{ts} I_{DC} AQ \tag{6}$$

where AP and AQ are the active and reactive power fractions, respectively, and V_{ts} is a terminal bus voltage of SMES unit (pu). The SMES active (P_{sm}) and reactive (Q_{sm}) power outputs are the output of the SMES controlled converter (CONV). The converter transfer function can be represented by the first-order time-lag compensator as

$$CONV = 1/(1 + 0.01s) \tag{7}$$

Here, $K_{Psm}(s)$ and $K_{Qsm}(s)$ are designed based on the proposed FGS-PID control.

3. **Proposed FGS-PID Controller.** It is well known that a PID controller is the most widely used in modern industry due to its simple control structure and easy design. The classical PID controller can be expressed in the time domain as

$$u_{PID}(t) = K_P e(t) + K_I \int e(t)dt + K_D \frac{de(t)}{dt} \tag{8}$$

where e is the input control signal of controller, $u_{PID}(t)$ is the control signal for the system, and K_P, K_I and K_D are the proportional, integral and derivative gains, respectively.

However, the classical PID controller does not yield reasonable performance over a wide range of operating conditions because of the fixed PID gains. This is the reason to use the fuzzy logic to tune the parameters of PID controller.

From (8), three coefficients K_P, K_I and K_D are tuned by using knowledge base and fuzzy interface of fuzzy gain scheduler, then the classical PID controller generates the control signal. The proposed FGS-PID controller scheme can be shown in Figure 3.

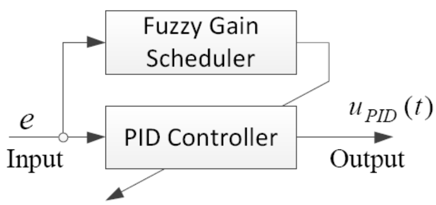

FIGURE 3. Schematic of FGS-PID controller

Through fuzzy knowledge, the online self-tuning PID parameters of FGS-PID controller can be established by the following equations

$$K_P = K_{PC}.K_{PF} \tag{9}$$

$$K_I = K_{IC}.K_{IF} \tag{10}$$

$$K_D = K_{DC}.K_{DF} \tag{11}$$

where K_{PC}, K_{IC} and K_{DC} are the proportional, integral and derivative gains of the classical PID controller, respectively. These PID gains are optimally tuned. K_{PF}, K_{IF} and K_{DF} are the proportional, integral and derivative gains, respectively. These gains are obtained from the online tuning of fuzzy gain scheduler.

From (9), (10) and (11), K_P, K_I and K_D are online tuned based on the current absolute error ($|E|$) and the current absolute derivative error ($|E'|$) by a fuzzy gain scheduler as shown in Figure 4. Note that the fuzzy gain scheduler has two inputs and three outputs. For the part of input, E and E' are given by

$$E = eK_{S1} \tag{12}$$

$$E' = e'K_{S2} \tag{13}$$

where K_{S1} and K_{S2} are the SF of fuzzy gain scheduler.

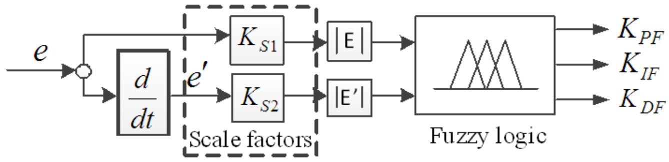

FIGURE 4. Block diagram of fuzzy gain scheduler

Here, the fuzzy gain schedule is based on the fuzzy singleton. The CRs of fuzzy gain scheduler are in the form of

$$\text{If input1 is } F \text{ and input2 is } G, \text{ then } K_{PF} = H, \ K_{IF} = I, \ K_{DF} = J \tag{14}$$

where F, G, H, I and J are the fuzzy set on the corresponding supporting sets. The MFs of these fuzzy sets for input and output are shown in Figure 5. The MFs for input1 and input2 as indicated in Figure 5(a), each input consists of three triangular memberships and one trapezoidal membership. Each output of the fuzzy gain scheduler includes three constant memberships that are S, M and L. From Figure 5, Z is zero, S is small, M is medium and L is large.

In case of the design of FGS-PID controller, there are two tuning parameters of SF, i.e., K_{S1} and K_{S2}. Besides, there are many tuning parameters of MFs and CRs. Here, consider two shapes of an input MF, i.e., triangular and trapezoidal memberships which are shown in Figure 6. A triangular membership is defined by three parameters, i.e., left base (L), center (C), and right base (R). For a trapezoidal membership, it is defined by four parameters, i.e., left base (L), center 1 (C_1), center 2 (C_2), and right base (R). Each input MF is composed of one trapezoidal membership and three triangular memberships. Each output MF includes three constant memberships. Accordingly, it has thirteen parameters for input and three parameters for output. One FGS-PID controller has two inputs and three outputs. Therefore, there are thirty five tuning parameters ($13 \times 2 + 3 \times 3 = 35$).

The CRs for two-inputs and one-output fuzzy logic controller, is represented by n rows and five columns matrix as shown in Figure 7. When this idea is applied to the fuzzy logic toolbox, n is the total number of relationships between all possible input pairs (for 4 MFs, $n = 4^2 = 16$). The third-fifth columns in the control rule table are the linguistic variable outputs. Generally, it is represented by a numeric symbol. The universe of discourse in this study contains seven memberships. Consequently, the control rules are represented by four numbers (1 to 4), 1: Z, 2: S, 3: M and 4: L. Note that there are sixteen tuning parameters. Hence, the total parameters for two inputs and three outputs of FGS-PID controller are fifty three ($2 + 35 + 16 = 53$).

In the FGS-PID controller design, the important procedure is how to determine the SFs, MFs and CRs. In general, they are determined by trial and error and designer's experiences. To solve this problem, this study applies a BCO algorithm to automatically determine the SFs, MFs and CRs.

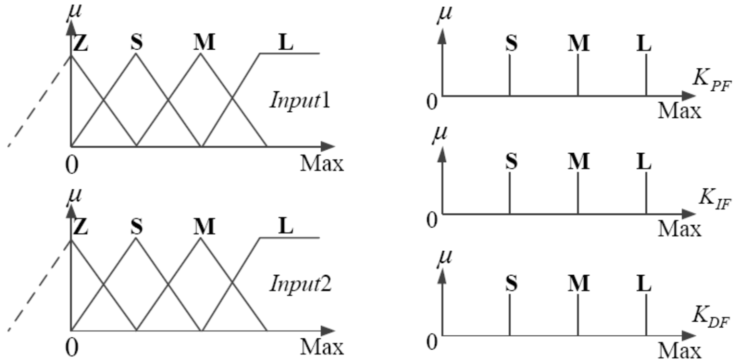

(a) Input (b) Output

FIGURE 5. Membership functions for input and output of FGS

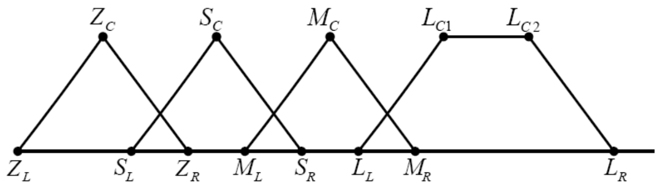

FIGURE 6. The shape of input membership functions

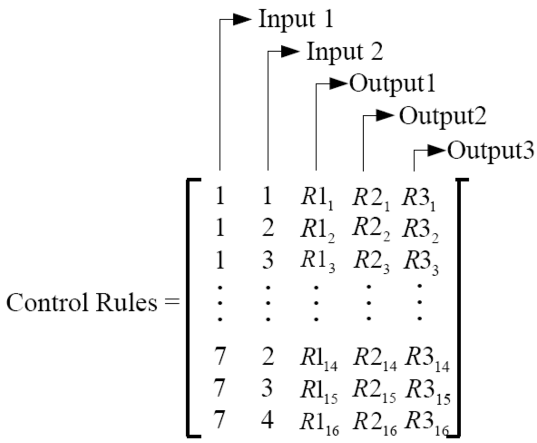

FIGURE 7. Structure of control rules for FGS-PID

The motivation of the practical use of the theoretic results of proposed method is the automatic optimization of SFs, MFs and CRs for the FGS-PID controller by BCO. Without trial and error and designer's experience, the optimal FGS-PID controller can be achieved. In addition, the proposed method can be practically applied in industries or power systems such as a self-learning support system for pupils based on a fuzzy scheme [29]. The application of proposed method to these practical systems not only considerably simplifies the control design process, but also significantly enhances the control effect of the system.

The novel and significant contribution of proposed BCO based FGS-PID controller of SMES for power system stabilization are given as follows.

1) The proposed FGS-PID controller is very effective and robust because the FGS-PID can deal with intrinsic uncertainties by changing controller parameters. The effectiveness and robustness of the proposed FGS-PID controller have been shown in simulation study.

2) Without trial and error, all adjusting parameters of the FGS-PID controller, i.e., SFs, MFs and CRs are automatically optimized by a BCO.

The optimization problem for the optimal FGS-PID controller is formulated based on the minimization of integral absolute error (IAE) of the speed difference between generators G1 and G3 ($\Delta\omega_d$) which implies the inter-area oscillation as,

$$\text{Minimize } IAE = \int_0^t |\Delta\omega_d|\, dt \tag{15}$$

This optimization problem is solved by the BCO.

4. **Bee Colony Optimization.** The BCO algorithm mimics the food foraging behaviour of swarms of honey bees [27]. Honey bees use several mechanisms like waggle dance to optimally locate food sources and to search new ones. This makes them a good candidate for developing new intelligent search algorithms. It is a very simple, robust and population based stochastic optimization algorithm. The procedure of the BCO algorithm for tuning FGS-PID parameters as shown in Figure 8 can be described as below:

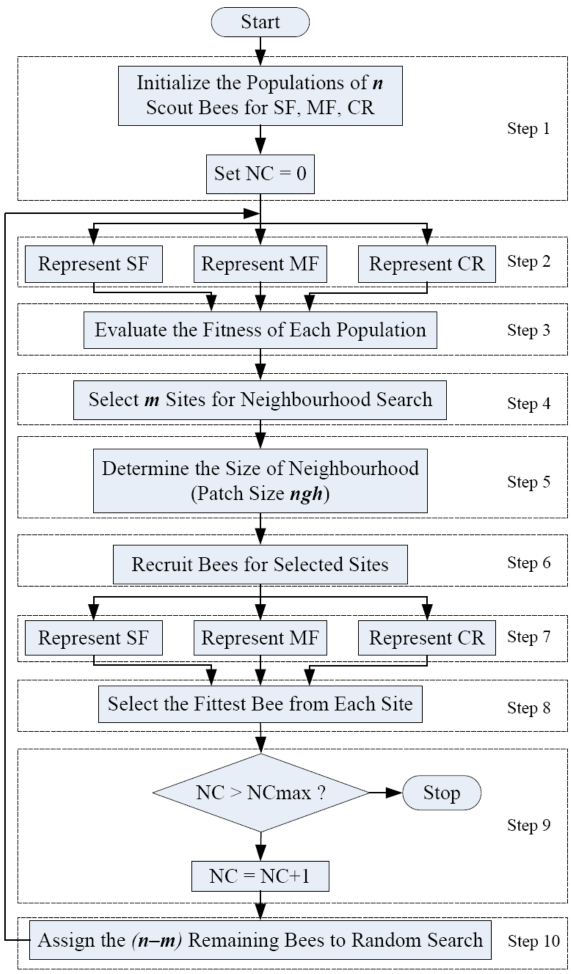

Figure 8. Procedure of BCO algorithm for tuning FGS-PID parameters

Step 1: Generate randomly the initial populations of n scout bees for the parameters of SF, MF and CR. These initial populations must be feasible candidate solutions that satisfy the constraints. Set $NC = 0$.

Step 2: Represent the value of SF, MF and CR from each population.

Step 3: Evaluate the fitness value of the initial populations by (15).

Step 4: Select m best sites for neighbourhood search. Separate the m best sites to two groups, the first group has e best sites and another group has $m - e$ best sites.

Step 5: Determine the size of neighbourhood search of each best size (patch size, ngh).

Step 6: Recruit bees of ne employed bees for selected sites (more bees for the best e sites).

Step 7: Represent the value of SF, MF and CR from each employed bee.

Step 8: Select the fittest bees from each patch.

Step 9: Check the stopping criterion. If satisfied, terminate the search, else $NC = NC + 1$.

Step 10: Assign the $n - m$ remaining bees to random search. Go to Step 2.

where ns is the number of scout bee, NC is the number of iteration, m is the number of sites selected for neighbourhood search, e is the number of best "elite" sites out of m selected sites and ne is the number of employed bee.

5. **Simulation Study.** The stabilizing effect of the SMES with an optimal FGS-PID controller is compared with the SMES with an optimal PID controller. Both controllers are optimized based on the same objective function (15) and the operating condition in case 1 as shown in Table 1. The constant parameters of BCO are set as: $ns = 100$, $ne = 20$, $m = 10$, $e = 5$, $ngh = 20\%$ and $NC = 100$.

As a result, the convergence curves of the SMES with the optimal PID controller and the SMES with the optimal FGS-PID controller are depicted in Figure 9. They start at the different initial values and gradually decrease to the minimum values.

The optimized parameters of $K_{Psm}(s)$ and $K_{Qsm}(s)$ of SMES with optimal FGS-PID controller are given in Table 2. Besides, the MFs and CRs of $K_{Psm}(s)$ and $K_{Qsm}(s)$ are shown in Figures 10 and 11 and Figures 12 and 13, respectively. For the compared optimal PID controller, the optimized parameters are given in Table 3.

Nonlinear simulations are carried out for four case studies in Table 1.

Table 1. Operating conditions and disturbances

Case	Applied Disturbance	Initial value of P_{T12} (pu)
1	Temporary 3 phases fault occurs at bus 13 for 70 ms and is cleared naturally.	3.0
2	Temporary 3 phases fault occurs on one line between bus 3 and 101 for 70 ms and is cleared naturally.	2.0
3	Loss of one line between bus 101 and 13 at $t = 0.5$ s	4.0
4	Temporary 3 phases fault occurs at bus 13 for 100ms and is cleared naturally.	vary from 2.5 to 4.5

Table 2. Optimized control parameters of FGS-PID controller

Controller	K_{S1}	K_{S2}	MF	CR
$K_{Psm}(s)$	0.886	0.932	Figure 8	Figure 9
$K_{Qsm}(s)$	1.245	1.043	Figure 10	Figure 11

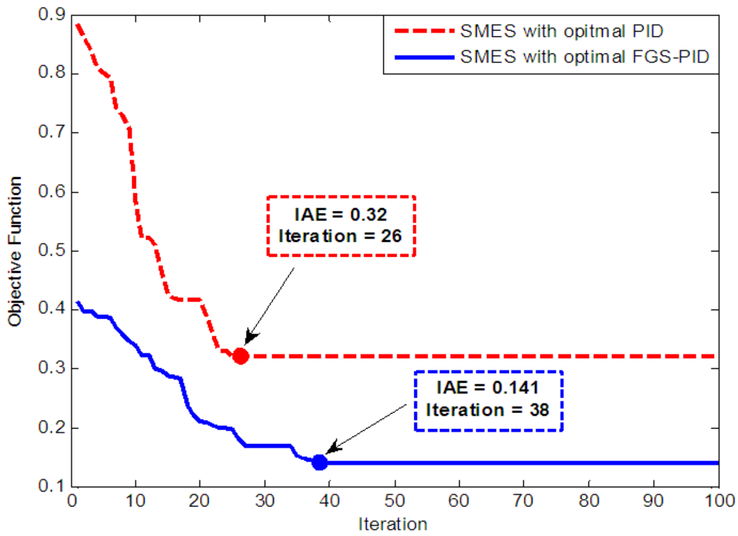

FIGURE 9. Convergence curves

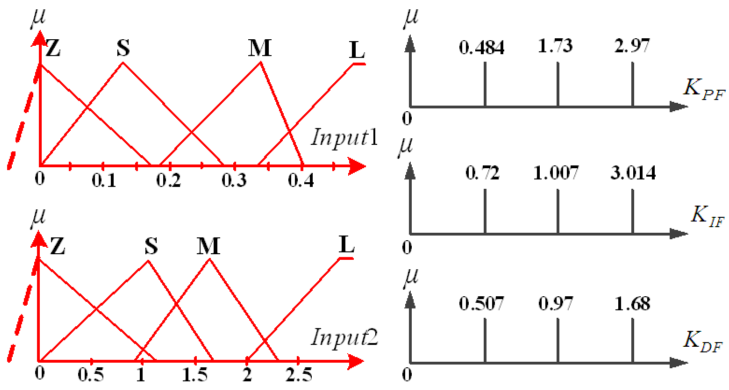

FIGURE 10. Optimized membership functions of $K_{Psm}(s)$

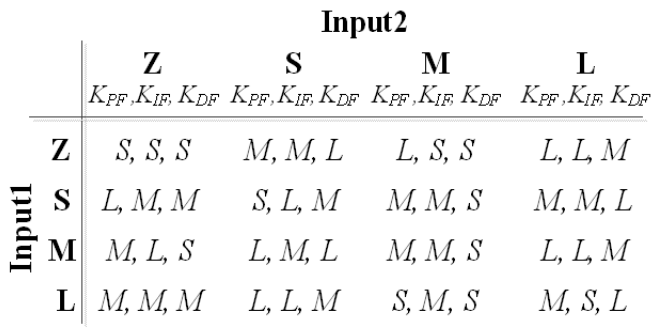

Input1 \ Input2	Z (K_{PF}, K_{IF}, K_{DF})	S (K_{PF}, K_{IF}, K_{DF})	M (K_{PF}, K_{IF}, K_{DF})	L (K_{PF}, K_{IF}, K_{DF})
Z	S, S, S	M, M, L	L, S, S	L, L, M
S	L, M, M	S, L, M	M, M, S	M, M, L
M	M, L, S	L, M, L	M, M, S	L, L, M
L	M, M, M	L, L, M	S, M, S	M, S, L

FIGURE 11. Optimized control rules of $K_{Psm}(s)$

TABLE 3. Optimized control parameters of PID controller

Controller	K_{PC}	K_{IC}	K_{DC}
Active power	5.701	1.82	0.044
Reactive Power	2.594	1.796	0.0063

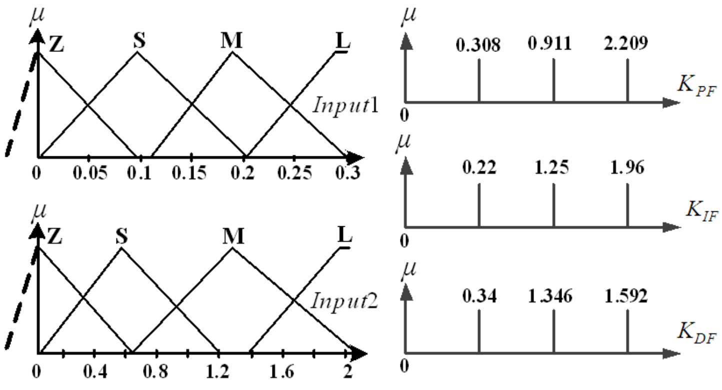

FIGURE 12. Optimized membership functions of $K_{Qsm}(s)$

Input1 \ Input2	Z (K_{PF}, K_{IF}, K_{DF})	S (K_{PF}, K_{IF}, K_{DF})	M (K_{PF}, K_{IF}, K_{DF})	L (K_{PF}, K_{IF}, K_{DF})
Z	*S, S, L*	*M, L, L*	*M, S, S*	*M, M, M*
S	*L, S, S*	*S, L, L*	*S, S, M*	*L, L, M*
M	*M, M, M*	*M, M, M*	*L, M, L*	*M, S, M*
L	*S, M, M*	*M, L, M*	*M, M, L*	*M, M, M*

FIGURE 13. Optimized control rules of $K_{Qsm}(s)$

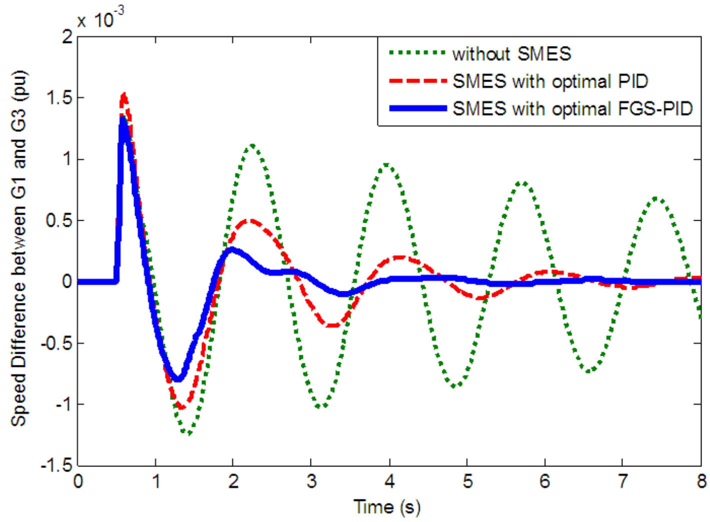

FIGURE 14. Generator speed difference between G1 and G3 in case 1

Simulation result of the generator speed difference between G1 and G3 in case 1 is depicted in Figure 14. Without SMES, after the fault occurs, the speed difference severely fluctuates. On the other hand, the SMES with optimal PID controller or optimal FGS-PID controller can alleviate the fluctuation considerably. Nevertheless, the SMES with optimal FGS-PID controller provides better damping effect than the SMES with optimal PID controller.

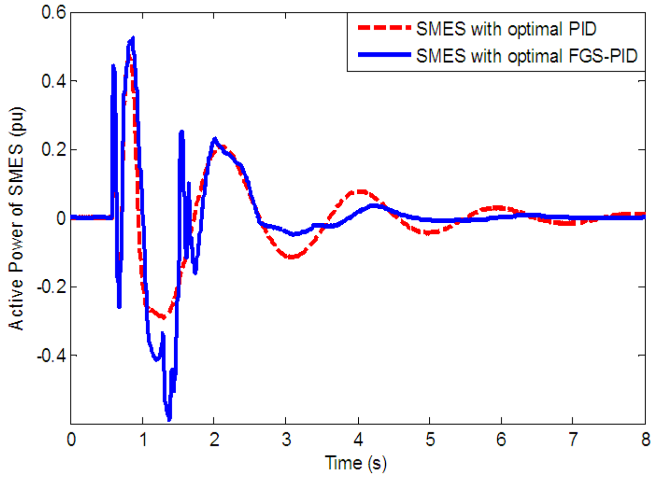

(a) Active power output of SMES

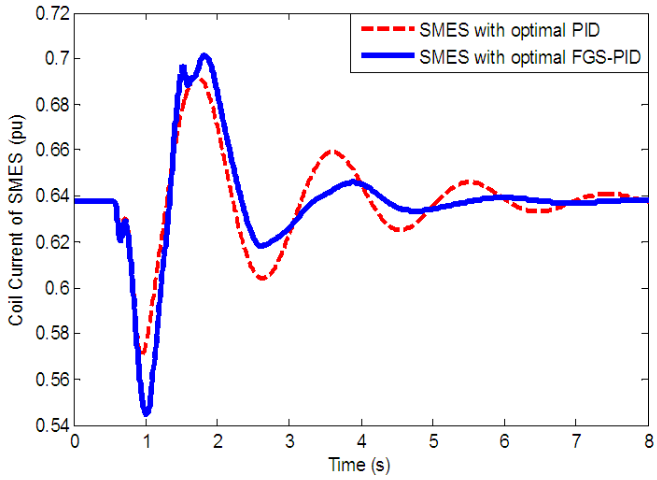

(b) Coil current of SMES

FIGURE 15. Active power output and coil current of SMES in case 1

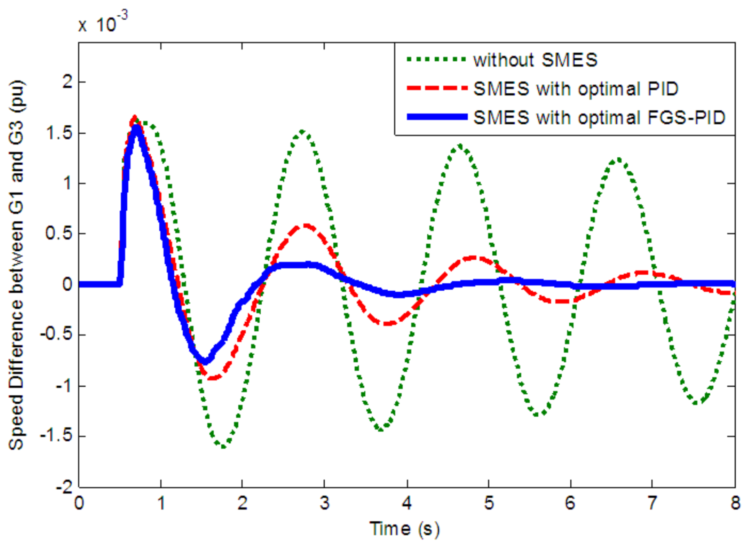

FIGURE 16. Generator speed difference between G1 and G3 in case 2

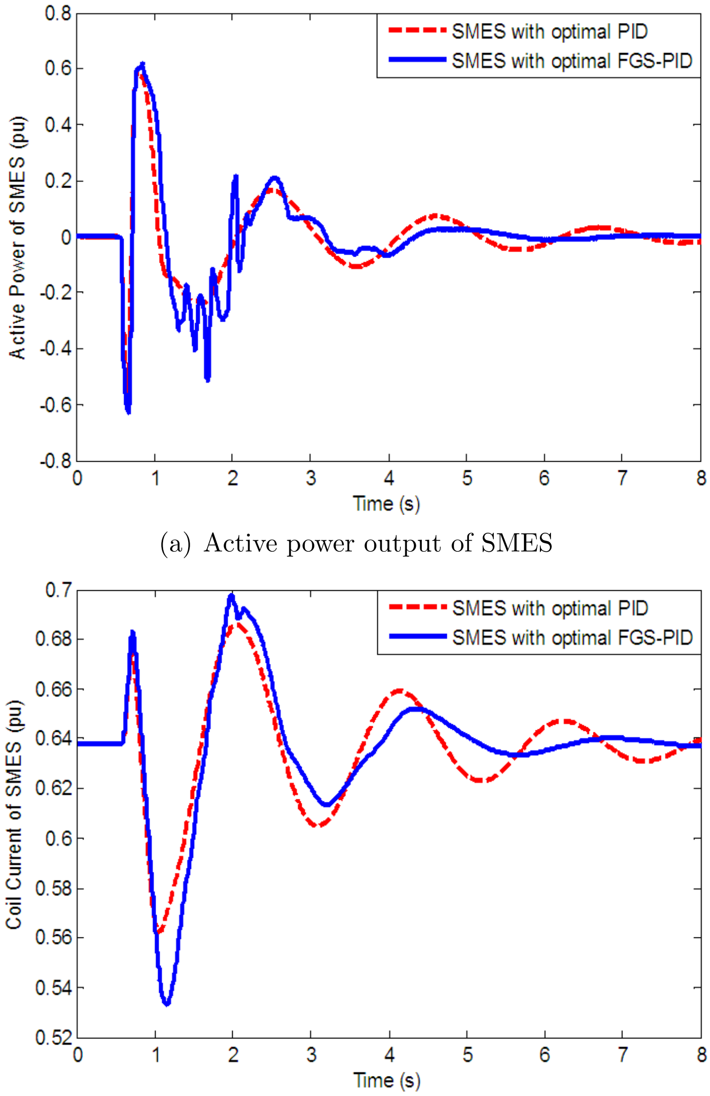

(a) Active power output of SMES

(b) Coil current of SMES

FIGURE 17. Active power output and coil current of SMES in case 2

The active power output and the coil current of SMES are demonstrated in Figures 15(a) and 15(b), respectively. It can be observed that the fluctuation of active power output and coil current of the SMES with optimal FGS-PID controller is higher than that of the EZ with optimal PID controller. Accordingly, the generator speed difference between G1 and G3 in case of the EZ with optimal FGS-PID controller are lower than that of the SMES with optimal PID controller.

For case 2, simulation results are shown in Figures 16 and 17. In comparison to the SMES with optimal PID controller, the SMES with optimal FGS-PID controller shows better stabilizing effect.

For case 3, simulation results are shown in Figures 18 and 19. The SMES with optimal PID controller completely loses stabilizing effect. The system becomes unstable same as the without SMES case. On the contrary, the proposed SMES with optimal FGS-PID controller can tolerate this severe disturbance. It is able to damp out power oscillations robustly. The active power output and coil current of SMES are demonstrated in Figures 18 (a) and (b), respectively.

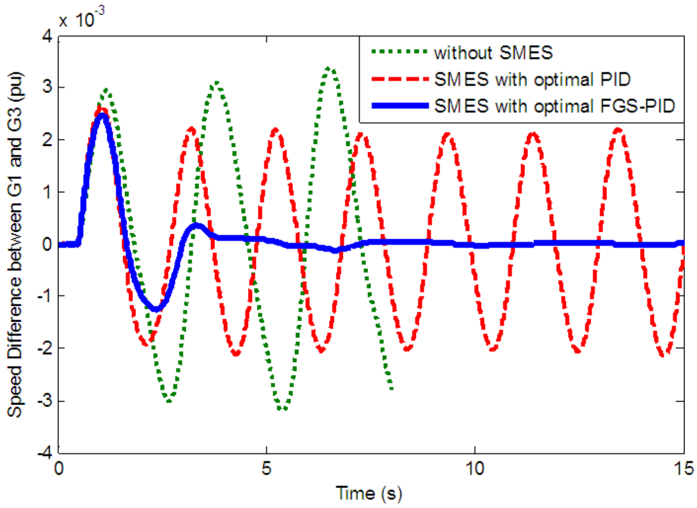

FIGURE 18. Generator speed difference between G1 and G3 in case 3

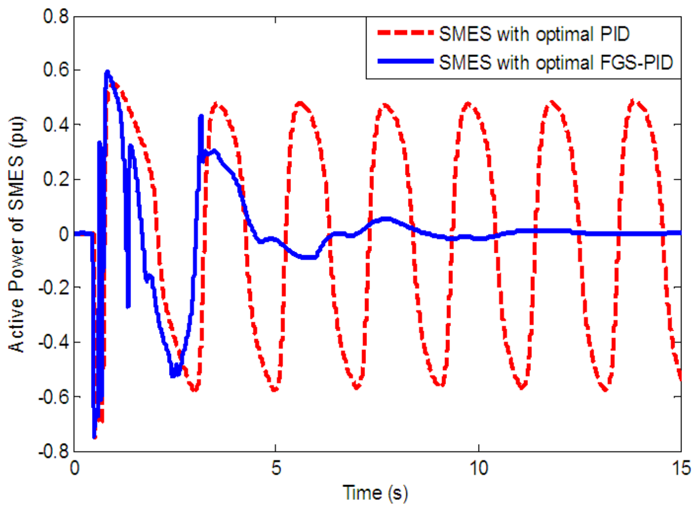

(a) Active power output of SMES

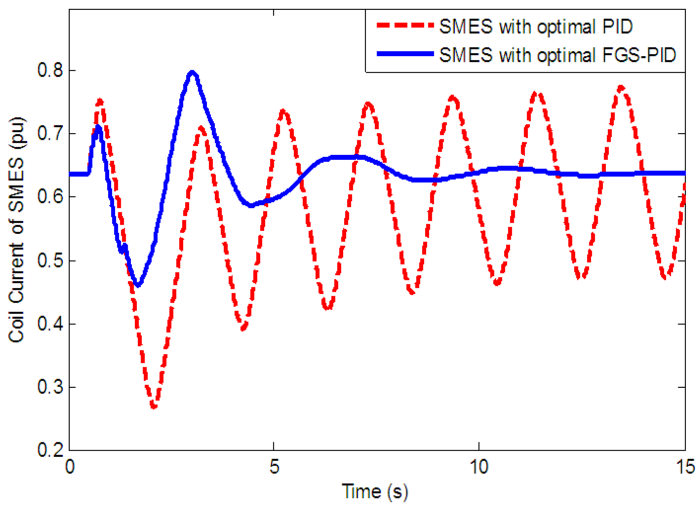

(b) Coil current of SMES

FIGURE 19. Active power output and coil current of SMES in case 3

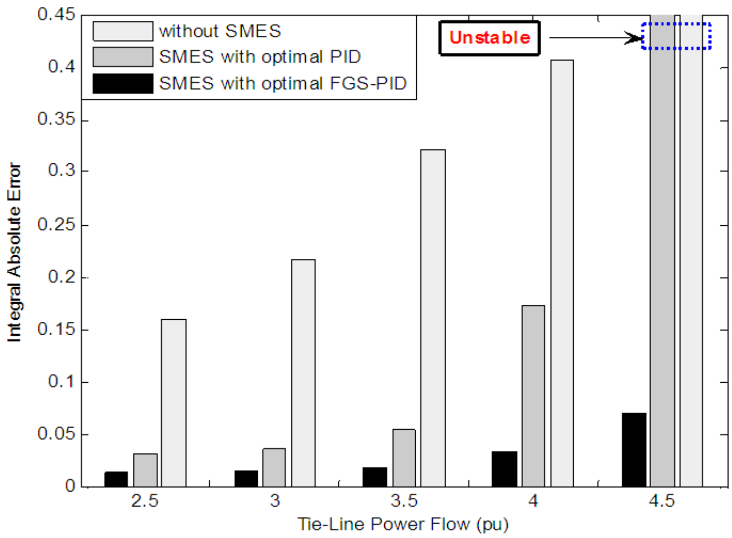

FIGURE 20. Integral absolute error of $\Delta\omega_d$ in case 4

In case 4, the initial tie-line power flow is varied under the occurrence of fault. The variation of IAE of the generator speed difference between G1 and G3 is shown in Figure 20. When the power flow increases, the IAE in case of without SMES and the SMES with optimal PID controller extremely increase. Eventually, the system becomes unstable when the initial tie-line power flow is at 4.5 pu. On the other hand, the IAE in case of SMES with optimal FGS-PID controller increases slightly. These results confirm that the superior robustness of the proposed SMES with optimal FGS-PID controller over the SMES with optimal PID controller against the heavy power flow.

6. **Conclusion.** The optimal fuzzy gain scheduling of the online self-tuning PID controller design for the SMES has been proposed for power system stabilization. The study results can be summarized as follows:

1) Without trial and error and designer's experience, the scale factors, membership functions and control rules of the optimal FGS-PID controller are automatically tuned by the BCO.
2) With the FLS-PID, the robustness of the PID controller against various system uncertainties and disturbances can be significantly improved since the PID parameters can be automatically tuned by the FGS according to the system operating conditions.

Simulation results confirm that the proposed SMES with an optimal FGS-PID controller is much superior to that of SMES with optimal PID controller in terms of stabilizing effect and robustness against severe faults and heavy power flow.

Acknowledgment. This work was supported by the King Mongkut's Institute of Technology Ladkrabang Research Fund.

REFERENCES

[1] P. Kundur, *Power System Stability and Control*, McGraw-Hill, 1994.

[2] J. Pahasa and I. Ngamroo, Least square support vector machine for power system stabilizer design using wide area phasor measurements, *International Journal of Innovative Computing, Information and Control*, vol.7, no.8, pp.4487-4501, 2011.

[3] Z. Cai, L. Zhu, Z. Lan, D. Gan, Y. Ni, L. Shi and T. Bi, A study on robust adaptive modulation controller for TCSC based on COI signal in interconnected power systems, *Electrical Power Systems Research*, vol.78, no.1, pp.147-157, 2008.
[4] X. Y. Bian, C. T. Tse, J. F. Zhang and K. W. Wang, Coordinated design of probabilistic PSS and SVC damping controllers, *International Journal of Electrical Power and Energy Systems*, vol.33, no.3, pp.445-452, 2011.
[5] I. Ngamroo, Simultaneous optimization of SMES coil size and control parameters for robust power system stabilization, *IEEE Trans. on Applied Superconductivity*, vol.21, no.3, pp.1358-1361, 2011.
[6] B. C. Pal, A. H. Coonick and D. C. Macdonald, Robust damping controller design in power system with superconducting magnetic energy storage devices, *IEEE Trans. on Power Systems*, vol.15, no.1, pp.320-325, 2000.
[7] B. C. Pal, A. H. Coonick, I. M. Jaimoukha and H. El-zobaidi, A linear matrix inequality approach to robust damping control design in power systems with superconducting magnetic energy storage device, *IEEE Trans. on Power Systems*, vol.15, no.1, pp.356-362, 2000.
[8] I. Ngamroo, C. Taeratanachai, S. Dechanupaprittha and Y. Mitani, Enhancement of load frequency stabilization effect of superconducting magnetic energy storage by static synchronous series compensator based on H_8 control, *Energy Conversion and Management*, vol.48, no.4, pp.1302-1312, 2007.
[9] A. H. M. A. Rahim and E. P. Nowicki, A robust damping controller for SMES using loop-shaping technique, *International Journal of Electrical Power & Energy Systems*, vol.27, no.5-6, pp.465-471, 2007.
[10] H. Shayeghi, A. Jalili and H. A. Shayanfar, A robust mixed H_2/H_∞ based LFC of a deregulated power system including SMES, *Energy Conversion and Management*, vol.49, no.10, pp.2656-2668, 2008.
[11] B. C. Pal, Robust pole placement versus root-locus approach in the context of damping interarea oscillations in power systems, *IEE Proc. Generation, Transmission and Distribution*, vol.149, no.6, pp.739-745, 2002.
[12] E. A. Gargari, R. Rajabioun, F. Hashemzadeh and F. R. Salmasi, A decentralized PID controller based on optimal shrinkage of Gershgorin bands and PID tuning using colonial competitive algorithm, *International Journal of Innovative Computing, Information and Control*, vol.5, no.10(A), pp.3227-3240, 2009.
[13] T. Hagiwara, K. Yamada, I. Murakami, Y. Ando and T. Sakanushi, A design method for robust stabilizing modified PID controllers for time-delay plants with uncertainty, *International Journal of Innovative Computing, Information and Control*, vol.5, no.10(B), pp.3553-3563, 2009.
[14] H. Yagi, J. Shimonishi, T. Yamamoto and T. Hinamoto, Design of a performance-adaptive PID controller with a model prediction structure, *International Journal of Innovative Computing, Information and Control*, vol.5, no.10(A), pp.2969-2983, 2009.
[15] C.-H. Hsieh, W.-H. Ho and J.-H. Chou, Optimal PID controllers design of PWM feedback time-varying systems using orthogonal-functions approach and genetic algorithm, *International Journal of Innovative Computing, Information and Control*, vol.5, no.2, pp.387-397, 2009.
[16] K. I. Hwu and Y. T. Yau, Performance enhancement of boost converter based on PID controller plus linear-to-nonlinear translator, *IEEE Trans. on Power Electronics*, vol.25, no.5, pp.1351-1361, 2010.
[17] W. Tan, Unified tuning of PID load frequency controller for power systems via IMC, *IEEE Trans. on Power Systems*, vol.25, no.1, pp.341-350, 2010.
[18] M. Santos and A. L. Dexter, Control of a cryogenic process using a fuzzy PID scheduler, *Control Engineering Practice*, vol.10, no.10, pp.1147-1152, 2002.
[19] N. W. Aung, E. W. Cooper, Y. Hoshino and K. Kamei, A proposal of fuzzy control systems for trailers driven by multiple motors in side slipways to haul out ships, *International Journal of Innovative Computing, Information and Control*, vol.3, no.4, pp.799-812, 2007.
[20] M. Wang, B. Chen and S. Tong, Adaptive fuzzy tracking control for strict-feedback nonlinear systems with unknown time delays, *International Journal of Innovative Computing, Information and Control*, vol.4, no.4, pp.829-837, 2008.
[21] L. Luoh, Control design of T-S fuzzy large-scale systems, *International Journal of Innovative Computing, Information and Control*, vol.5, no.9, pp.2869-2880, 2009.
[22] K. J. Astrom and B. Wittenmark, *Adaptive Control*, Addison-Wesley, Publishing Company, 1989.
[23] E. Cam and I. Kocaarslan, Load frequency control in two area power systems using fuzzy logic controller, *Energy Conversion and Management*, vol.46, no.2, pp.233-243, 2005.

[24] E. Cam and I. Kocaarslan, A fuzzy gain scheduling PI controller application for an interconnected electrical power system, *Electric Power Systems Research*, vol.73, no.3, pp.267-274, 2005.
[25] F. U. Syed, M. L. Kuang, M. Smith, S. Okubo and H. Ying, Fuzzy gain-scheduling proportional-integral control for improving engine power and speed behavior in a hybrid electric vehicle, *IEEE Trans. on Vehicular Technology*, vol.58, no.1, pp.69-84, 2009.
[26] L. H. Hassan, H. A. F. Mohamed, M. Moghavvemi and S. S. Yang, Automatic generation control of power system with fuzzy gain scheduling integral and derivative controllers, *International Journal of Power Energy and Artificial Intelligence*, vol.1, no.1, pp.29-33, 2008.
[27] D. Karaboga, An idea based on honey bee swarm for numerical optimization, *Technical Report-Tr06t, Erciyes Univ.*, Turkey, 2005.
[28] S. Dechanupaprittha, K. Hongesombut, M. Watanabe, Y. Mitani and I. Ngamroo, Stabilization of tie-line power flow by robust SMES controller for interconnected power system with wind farms, *IEEE Trans. on Applied Superconductivity*, vol.17, no.2, pp.2365-2368, 2007.
[29] K. Eguchi, S. Kurebayashi, H. Zhu, T. Inoue and F. Ueno, A self-learning support system for pupils based on a fuzzy scheme, *International Journal of Innovative Computing, Information and Control*, vol.4, no.10, pp.2441-2450, 2008.